European Journal of Radiology 120 (2019) 108689

Contents lists available at ScienceDirect

European Journal of Radiology

journal homepage: www.elsevier.com/locate/ejrad

Research article

Hyperintense nodule-in-nodule on hepatobiliary phase arising within hypovascular hypointense nodule: Outcome and rate of hypervascular transformation

Roberto Cannella[a,*], Alberto Calandra[a], Giuseppe Cabibbo[b], Massimo Midiri[a], An Tang[c], Giuseppe Brancatelli[a]

[a] Section of Radiology - BiND, University Hospital "Paolo Giaccone", Via del Vespro 129, 90127, Palermo, Italy
[b] Section of Gastroenterology & Hepatology, PROMISE, University of Palermo, Piazza delle Cliniche 2, 90127, Palermo, Italy
[c] Department of Radiology, Centre Hospitalier de l'Université de Montréal, 1000, rue Saint-Denis, Montréal, Québec, H2X 0C2, Canada

ARTICLE INFO

Keywords:
Nodule-in-nodule
Magnetic resonance imaging
Gadoxetate disodium
Hepatobiliary phase
Hepatocellular carcinoma

ABSTRACT

Purpose: To investigate the clinical implications and natural history of observations showing a "nodule-in-nodule" architecture on hepatobiliary phase (HBP) in a cirrhotic population.

Method: This is an IRB-approved retrospective study conducted in a single institution. We identified 20 patients (11 men and 9 women, mean age 71 years, range 51–83 years) who had a hyperintense nodule on HBP arising within a larger HBP-hypointense nodule without arterial phase hyperenhancement (APHE) at gadoxetate disodium-enhanced MRI. Size and signal intensity of the nodules were evaluated in all sequences, along with the evolution of the nodules at serial MRI studies.

Results: Twenty-four nodules were analyzed in 20 patients. Mean diameter of the inner hyperintense nodule on HBP was 1.1 cm (range 0.6–1.8 cm) and that of the outer hypovascular hypointense nodule was 2.1 cm (range 1.2–4.1 cm). All intranodular foci were hyperintense on HBP and showed a typical pattern for hepatocellular carcinoma (HCC) with APHE and washout on portal venous phase (PVP) (n = 11, 46%), washout only (n = 7, 29%) or APHE with no washout (n = 6, 25%). The hyperintensity on 3-, 5- and 10-minute phases was seen in 21%, 58% and 83% of the nodules, respectively. In twelve out of sixteen (75%) nodules with subsequent imaging available the hyperintensity on HBP occurred before either the appearance of APHE or washout on PVP.

Conclusions: HBP-hypointense nodules without APHE may contain a hyperintense smaller nodule-in-nodule on HBP that can precede the appearance of either APHE or washout on PVP.

1. Introduction

Hepatocellular carcinoma (HCC) is the second leading cause of cancer death worldwide [1], and is the final result of the progression of premalignant dysplastic nodules into early and progressed HCC [2]. Magnetic resonance imaging (MRI) has the ability to depict the vascular changes occurring in this process by demonstrating the appearance of a small, hypervascular focus arising within a larger hypovascular early HCC or dysplastic nodule. This condition has been described as the "nodule-in-nodule" architecture [3,4].

The introduction of hepatobiliary contrast agents has improved the detection of HCC on MRI. These contrast agents allow the radiologist to investigate at the same time imaging features related to changes in vascularity and altered function of the hepatic cells involved in the dedifferentiation process. Indeed, another event occurring in the multistep hepatocarcinogenesis process is the progressive loss of the organic anion transporting polypeptide (OATP) 1B3 carrier expression on the vascular pole of the hepatocyte membrane, which is responsible for the uptake of gadoxetate disodium. As a consequence, in 80–91% of cases, HCC appears as a hypointense lesion compared to the surrounding liver parenchyma on hepatobiliary phase (HBP), while in the remaining 9–20% HCCs show hyperintensity on HBP [5], due to the overexpression of uptake transporter OATP1B3. Indeed, there is a highly significant correlation between signal intensity of HCC on HBP and grade of OATP1B3 expression in HCC cells [6–8].

HBP-hypointense nodules without arterial phase hyperenhancement

Abbreviations: APHE, Arterial Phase Hyperenhancement; DWI, Diffusion Weighted Imaging; HBP, Hepatobiliary Phase; HCC, Hepatocellular Carcinoma; MRI, Magnetic Resonance Imaging; OATP, Organic Anion Transporting Polypeptide; PVP, Portal Venous Phase; TP, Transitional Phase

* Corresponding author at: Via del Vespro 129, 90127, Palermo, Italy.
E-mail address: rob.cannella@libero.it (R. Cannella).

https://doi.org/10.1016/j.ejrad.2019.108689
Received 6 June 2019; Received in revised form 4 September 2019; Accepted 18 September 2019

(APHE) have been reported in recent years as a condition at risk for evolving into hypervascular progressed HCC [8–12]. The majority of these HBP-hypointense nodules without APHE in high risk patients are already early HCCs which have lost the portal venous supply and have a reduced OATP1B3 carrier expression, but have not developed neoangiogenesis yet, accounting for the lack of hypervascularity on hepatic arterial phase. While evolution into progressed HCC is typically demonstrated by the occurrence of APHE within these HBP-hypointense nodules [12], in our clinical practice we have occasionally encountered patients in whom the appearance on hepatobiliary phase of a smaller hyperintense nodule within the larger hypointense nodule predated the occurrence of hypervascularity. In a prior study, Kobayashi et al. [13] reported that around one-third of hypervascular foci found within larger hypovascular high-risk borderline lesion (dysplastic nodule or early HCC) showed hyperintensity in larger HBP-hypointense nodules on gadoxetate disodium-enhanced MRI. However, this study was limited by the description of signal intensity on HBP only, by the lack of longitudinal evolution of these nodules and by the detection of the hypervascular inner nodule with CT hepatic arteriography, an invasive technique that is not routinely performed in Western countries. We hypothesized that, as a biomarker of the multistep hepatocarcinogenesis process, the hyperintense nodule-in-nodule could predate the occurrence of APHE, and therefore we tried to put this observation into proper clinical perspective by analyzing a population of cirrhotic patients in a defined time span.

Therefore, the purpose of this study was to retrospectively determine the spectrum of imaging findings and natural history of observations showing a “nodule-in-nodule” architecture on hepatobiliary phase in a cirrhotic population.

2. Materials and methods

Our institutional review board approved this retrospective study. The requirement for informed consent was waived due to its retrospective nature.

2.1. Population

Inclusion criteria included: 1) adult patients with cirrhosis primarily due to HCV (75%) or HBV (14%) infection, non-alcoholic steatohepatitis (10%) or alcohol abuse (1%); 2) gadoxetate disodium-enhanced MRI examination performed between January 2008 and December 2018; 3) technically adequate 20-minute HBP that was defined as a phase showing all the three following findings: T1-hyperintense parenchyma, contrast excretion through the biliary tree and hypointense vessels in comparison to the surrounding liver [14]; 4) presence of at least one nodule showing hyperintensity on HBP, regardless of its behavior on other phases/sequences; 5) presence of a larger hypointense nodule surrounding a smaller hyperintense nodule on hepatobiliary phase, defined as a nodule-in-nodule architecture on HBP. Lesion hypointensity on hepatobiliary phase was defined as a round solid nodule showing lower signal intensity in comparison to the surrounding background liver but higher signal in comparison to fluid/cyst.

An Author (A.C.) with 4 year of experience in abdominal radiology, not involved in final imaging interpretation, reviewed the gadoxetate disodium-enhanced MRI examinations to exclude patients with nodules showing only hyperintensity on HBP with the following imaging features (Fig. 1): 1) multiple and ≤ 1.5 cm nodules, with concurrent isointensity or spontaneous hyperintensity on pre-contrast T1-weighted images, not visible on T2-weighted and diffusion-weighted images, with no APHE and homogeneously hyperintense on hepatobiliary phase, and not surrounded by a larger hypointense nodule or by a rim of hypointensity on HBP, that are typically due to benign regenerative, dysplastic or FNH-like nodules (n = 113) [15]; or 2) > 1.0 cm hyperintense nodule on HBP showing both APHE and washout on portal venous phase, surrounded or not by a distinct rim of hypointensity on HBP, that correspond to HCC (n = 30). Of note, patients with co-existence of one of the above conditions with the presence of nodule-in-nodule architecture on HBP were not excluded from the final cohort.

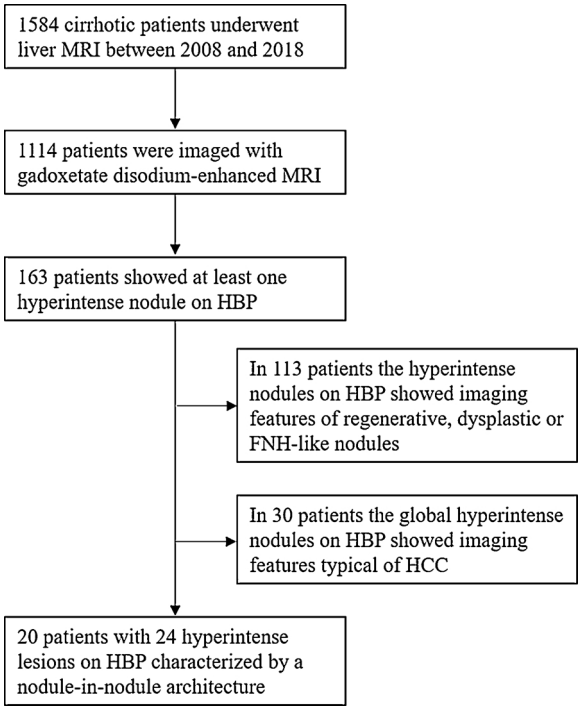

Fig. 1. Flow diagram for the selection of the final population.

We also collected demographic and clinical data of the patients, including etiology of cirrhosis, Child-Pugh score, prior history of HCC, systemic and loco-regional treatment for each patient.

The final population consisted of 20 patients with at least one hyperintense nodule-in-nodule on HPB, including eleven men and nine women, with a mean age of 71.2 ± 9.0 years (range 51–83 years). The etiologies of the underlying cirrhosis were HCV (n = 15), HBV (n = 4) or coinfection of HCV and HBV (n = 1). Fourteen patients had a Child-Pugh score A, while six presented a Child-Pugh B. A history of prior treated HCC was present in nine (45%) patients.

2.2. MRI technique

MRI examinations were performed on two 1.5 T scanners (Signa Excite, General Electric, Healthcare, Milwaukee, WI, USA; or Intera Achieva 1.5 Philips Healthcare, Best, The Netherlands) equipped with a 16-channel body phased-array coil.

The baseline imaging protocol (Table 1) for both scanners included axial T2-weighted turbo or fast spin-echo (with and without fat saturation) sequences and axial dual gradient-recalled echo (GRE) T1-weighted sequence (in-phase and opposed-phase). Axial T1-weighted three-dimensional GRE sequence with fat suppression (Liver Acquisition with Volume Acceleration, LAVA, General Electric or T1-weighted high-resolution isotropic volume examination, THRIVE; Philips Healthcare) were obtained before and after the administration of contrast agent.

A bolus of 0.025 mmol/Kg of gadoxetate disodium (Gd-EOB-DTPA, Primovist, Bayer Healtcare, Berlin, Germany) was injected at a rate of 1 mL/sec, followed by 20-mL saline flush at the same injection rate, using an automatic injector (Medrad® Spectris Solaris® EP, Bayer Healtcare, Berlin, Germany). An automated bolus detection algorithm (MR SmartPrep; GE Medical Systems) or fluoroscopic triggering (Bolus-Trak; Philips Medical Systems) was used to obtain an optimal hepatic arterial phase. Scanning delays after automatic detection of contrast bolus were 12–14 seconds, 50 s, 3 min, 5 min, 10 min and 20 min,

Table 1
Acquisition parameters at 1.5 T MRI scanners.

	Axial T2-weighted sequence	Axial T1-weighted Dual GRE (in and out of phase)	Axial T1-weighted 3D GRE Unenhanced and Contrast-Enhanced	Diffusion Weighted Imaging
1.5 T MR Signa Excite, GE Healthcare				
TR (ms)	1800-2400	150	3.8	1400
TE (ms)	47-65	2.2/4.5	1.8	76
FA (degrees)	90	70	12	90
Number of slides	33-38	66-74	92-116	33-36
Slice Thickness (mm)	6	4	4.4	6
Reconstruction Interval (mm)	7	5	2.2	7
Acquisition Matrix	256 × 224	256 × 160	256 × 256	144 × 192
FOV (cm)	35-40 × 35-40	35-40 × 35-40	35-40 × 35-40	35-40 × 35-40
NEX	4	1	0.71	2
1.5 T MR Intera Achieva, Philips Healthcare				
TR (ms)	1073-3000	100	4.4	2195
TE (ms)	80-200	2.3/4.6	2.1	57
FA (degrees)	90	80	10	90
Number of slides	28-36	60-72	83-110	116-140
Slice Thickness (mm)	6	4.5	5	7
Reconstruction Interval (mm)	7	2.5	2.3	7
Acquisition Matrix	268-252 × 206-144	188 × 156	270 × 188	108 × 81
FOV (cm)	35-40 × 35-40	35-40 × 35-40	35-40 × 35-40	35-40 × 35-40
NEX	2	1	1	2

TR: Repetition Time; TE: Echo Time; FA: Flip Angle; FOV: Field of View; NEW: number of excitations.

respectively, for the acquisition of the late hepatic arterial, portal venous phase (PVP), multiple transitional (TP) and hepatobiliary phases. The respiratory-triggered, fat-suppressed, T2-weighted fast spin-echo sequence and axial diffusion-weighted imaging (DWI) sequences were obtained between the 3-minute transitional phase and the hepatobiliary phase. DWI sequence were acquired with *b* values of 0, 150 and 800 s/mm^2.

2.3. MRI analysis

The gadoxetate disodium-enhanced MRI examinations were reviewed retrospectively and jointly by two abdominal radiologists (G.B. and R.C. with 19 and 5 years of experience in abdominal imaging, respectively). The latest MRI was selected as index exam for qualitative analysis of untreated nodules. The number, size and signal intensity of the nodules relative to the background liver were evaluated. The nodule size was measured as the largest axial diameter of the inner HBP-hyperintense and of the outer HBP-hypointense nodules without APHE. The MRI signal intensity of the inner and outer nodules was qualitatively compared with the background liver parenchyma and it was scored as hypointense, isointense or hyperintense on T2-weighted and DWI sequences, along with the dynamic post-contrast, transitional and hepatobiliary phases. When a lesion already showed high signal intensity on pre-contrast T1-weighted images and the radiologists could not determine with confidence whether the nodules were enhancing or not after contrast injection, subtracted images were evaluated. With regard to T2-weighted signal, a nodule was defined as slightly hyperintense when the signal was higher than the liver but lower or equal to the spleen, and markedly hyperintense when the signal was higher than that of the spleen. A nodule was considered as typical HCC when the following imaging criteria were observed: i) size of the nodule larger than 1 cm; ii) nonrim APHE; iii) washout on portal venous phase [16].

In patients who had follow-up with gadoxetate disodium-enhanced MRI, the reviewers assessed size stability of the nodules and changes in signal intensity and appearance of either APHE or washout on PVP. Substantial growth was defined as ≥ 50% size increase in ≤ 6 months [16].

2.4. Statistical analysis

Data of final population and qualitative MRI analysis were reported as continuous variables, summarized using mean and standard deviation with range or median and interquartile range (IQR) depending on Shapiro-Wilk normality test, or categorical variables using counts and percentages. Differences in nodules' characteristics according to the dynamic MRI pattern (i.e. APHE and washout on PVP) and the evolution were assessed using the independent samples *t*-test for normally distributed continuous variables (size of the nodules) and the Pearson $\chi 2$ or Fisher exact test for categorical variables.

Statistical significance level was set at $p < 0.05$. Statistical analysis was conducted by using SPSS software (Version 20.0. Armonk, NY, USA: IBM Corp).

3. Results

A total of 24 hyperintense nodules arising within a larger HBP-hypointense nodule without APHE were identified in 20 patients. The prevalence of patients with these nodules in our cohort was 1.2%. Sixteen patients had one nodule, while four patients had two nodules each.

3.1. Nodules size and signal intensity

Mean diameter of the outer HBP-hypointense nodules without APHE was 2.1 ± 0.6 cm (range 1.2–4.1 cm), while the diameter of the inner HBP-hyperintense nodules was 1.1 ± 0.2 cm (range 0.6–1.8 cm). The outer nodules already showed hypointensity in comparison to the background liver in 46% of cases ($n = 11$) on PVP, in 87% ($n = 21$) on 3-minute and in 100% ($n = 24$) on 5-minutes TP. All the outer nodules were also hypointense on 10-minute and 20-minute HBP. The imaging characteristics at index MRI examinations of the inner nodules are summarized in Table 2. After the injection of gadoxetate disodium, 11 (46%) inner HBP-hyperintense nodules showed a typical pattern for HCC with APHE and washout on PVP. In the 13 (54%) remaining nodules the vascular enhancement pattern of the inner nodule was atypical for HCC, showing only washout appearance on PVP ($n = 7$, 29%) or APHE with no washout ($n = 6$, 25%). There was no difference in size of the inner nodules with APHE (1.1 ± 0.2 vs 1.1 ± 0.3, $p = 0.718$)

Table 2
MRI signal intensity of the inner nodule in nodule with gadoxetate disodium.

	MRI signal intensity of the inner nodule		
MRI Sequences	Hyperintense	Isointense	Hypointense
T2-weighted imaging	5 (21)	18 (75)	1 (4)
Hepatic arterial phase	17 (71)	7 (29)	0 (0)
Portal venous phase	0 (0)	6 (25)	18 (75)
3-minute phase	5 (21)	8 (33)	11 (46)
5-minute phase	14 (58)	6 (25)	4 (17)
10-minute phase	20 (83)	3 (13)	1 (4)
20-minute hepatobiliary phase	24 (100)	0 (0)	0 (0)

Numbers are number of nodules, numbers in parentheses are percentages.

or washout on PVP (1.0 ± 0.2 vs 1.2 ± 0.3, p = 0.349) compared to inner nodules without these imaging features. On later phases, five (21%) inner nodules were already hyperintense on 3-minute TP, 14 (58%) nodules became hyperintense on 5-minute TP, while 20 (83%) nodules showed hyperintensity 10 min after the contrast injection. All 24 inner nodules were hyperintense on 20-minute HBP (Figs. 2 and 3). On T2-weighted images they were most commonly isointense (n = 18, 75%). DWI was available in 13 patients and in four cases restricted diffusion of the inner nodules was noted.

3.2. Natural history and fate of the nodules

While for eight nodules no serial imaging was available, subsequent gadoxetate disodium-enhanced MRI examinations were available for 16 nodules in 14 patients. The median length of follow-up was 368 days (IQR 245–755 days; mean number of follow-up MRI: 3; range 2–5 MRIs). Fourteen out of 16 (87%) nodules were already hyperintense on previous examinations, while two nodules were hypointense. At follow-up we observed the appearance of either arterial phase hyperenhancement (n = 4, 25%, with median interval of 565 days, IQR 198–1003 days), washout on PVP (n = 2, 12.5%, 220 and 232 days) or appearance of both APHE and washout on PVP (n = 6, 37.5%, median

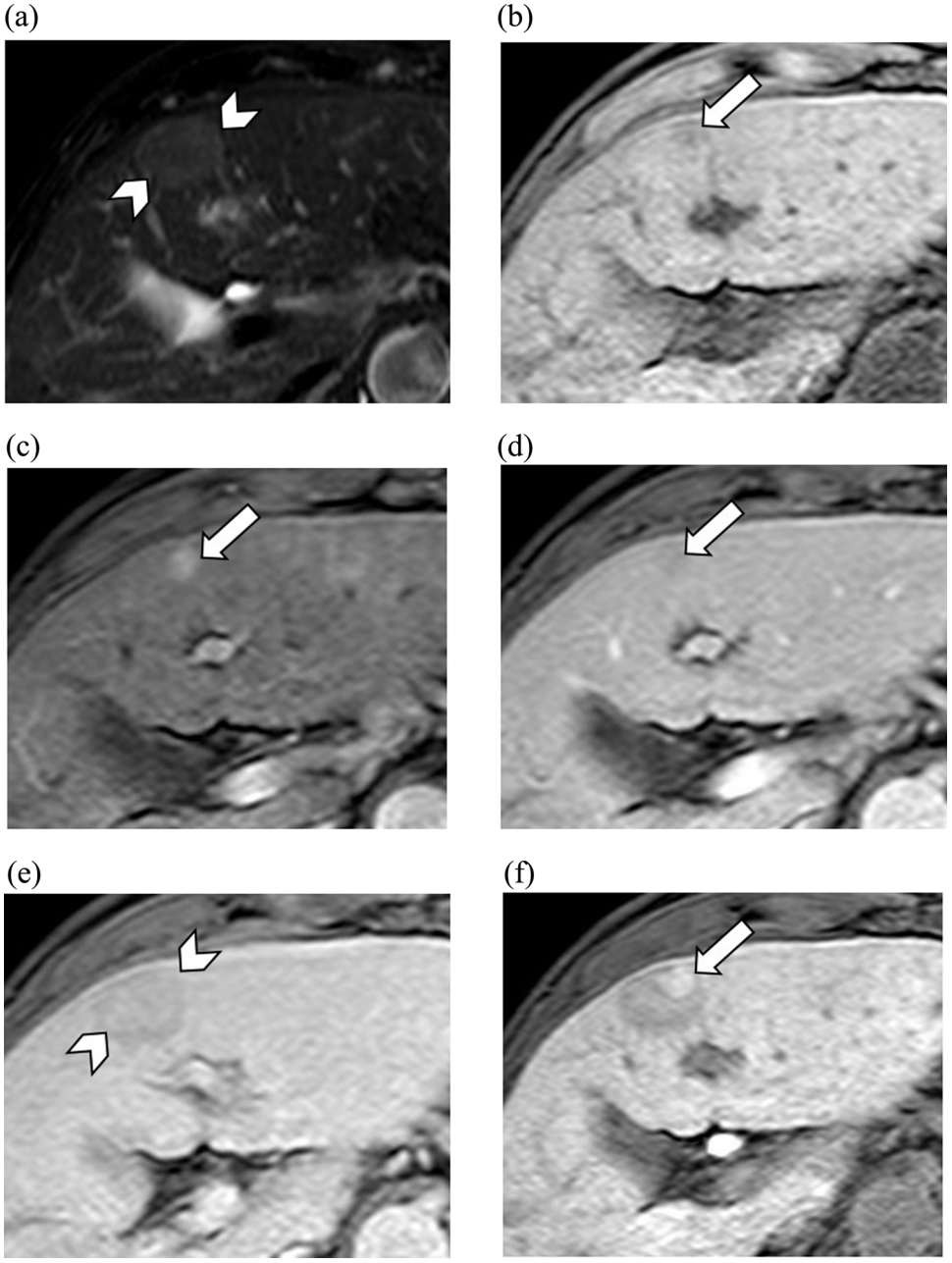

Fig. 2. 80-year-old man with HCV-related cirrhosis imaged with gadoxetate disodium-enhanced MRI. Smaller nodule (arrows) measuring 1.3 cm within a larger 2.8 cm nodule (arrowheads) in segment IV corresponding to nodule-in-nodule architecture. **(a)** Mild T2 hyperintensity of the nodule. The peripheral inner nodule within the larger nodule is hypointense on **(b)** pre-contrast T1-weighted image and shows **(c)** arterial phase hyperenhancement and **(d)** washout on portal venous phase. The outer larger nodule becomes **(e)** hypointense on 3-minute transitional phase. **(f)** A nodule-in-nodule architecture is demonstrated on hepatobiliary phase. Notice how the larger HBP-hypointense nodule without APHE is visible on transitional and hepatobiliary phase only.

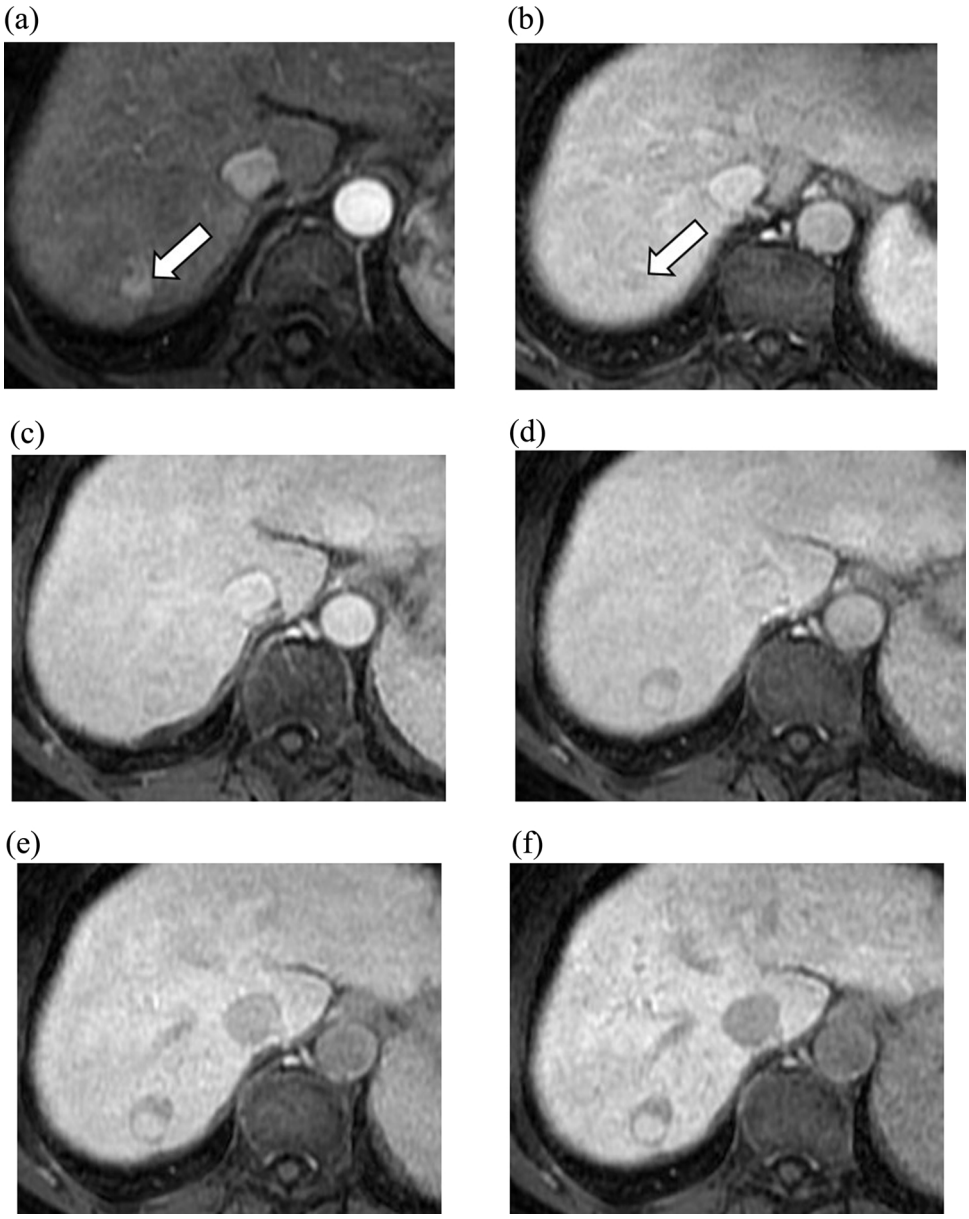

Fig. 3. 65-year-old woman with HCV-related cirrhosis. Gadoxetate disodium-enhanced MRI shows a 1.0 cm nodule (arrow) in segment VII. **(a)** Arterial phase hyperenhancement, **(b)** washout on portal venous phase **(c)** and hypointensity at 3-minute transitional phase of the nodule. This corresponds to a nodule-in-nodule architecture that is already hyperintense on **(d)** 5-minute transitional phase, **(e)** at 10-minute phase and **(f)** persists on 20-minutes hepatobiliary phase.

385 days, IQR 83–485 days). Therefore, in twelve (75%) of sixteen nodules, hyperintensity on HPB occurred before (median 315 days, IQR 124–538 days) the appearance of either APHE or washout on PVP (Fig. 4). History of prior HCC was significantly more common in nodules with appearance of either APHE or washout on PVP on subsequent MRI examinations (n = 9, 75% vs n = 0, 0%, p = 0.019).

A clinical follow-up was available in 16 patients with 19 nodule-in-nodules, while in four patients with five lesions clinical data were not available. All nodules either had locoregional (transarterial chemoembolization [TACE], n = 9; radiofrequency ablation [RFA] n = 5; percutaneous ethanol injection [PEI], n = 2) or systemic treatment with anti-angiogenetic drugs (Sorafenib, Nexavar, Bayer Healthcare, Germany) due to development of multifocal HCC (n = 3). In two patients we observed the appearance of a new nodule-in-nodule in a different liver segment with similar imaging features to the ones that were previously treated, 258 and 459 days after RFA and TACE, respectively.

4. Discussion

HBP-hypointense nodules without APHE have a significant risk for development of hypervascularity, which is a key criterion for the non-invasive diagnosis of HCC, with a pooled rate of 28% for hypervascular transformation [12]. Our cohort included lesions consisting of an outer HBP-hypointense nodule without APHE with a mean diameter larger than 2 cm and demonstrating hypointensity on PVP, 3-minute, 5-minute and subsequent phases in 46%, 87% and in 100% of cases, respectively. Moreover, prior history of HCC was noted in 45% of our patients. These baseline characteristics may have contributed to the high prevalence of hypervascularity since recent evidences have shown how larger size and prior history or HCC are both conditions significantly increasing the likelihood for development of HCC [10,12,17–19].

The nodule-in-nodule architecture is an uncommon imaging feature occurring in approximately 3–6% of patients with hypovascular high-risk nodules [20,21]. We undertook this study to investigate the

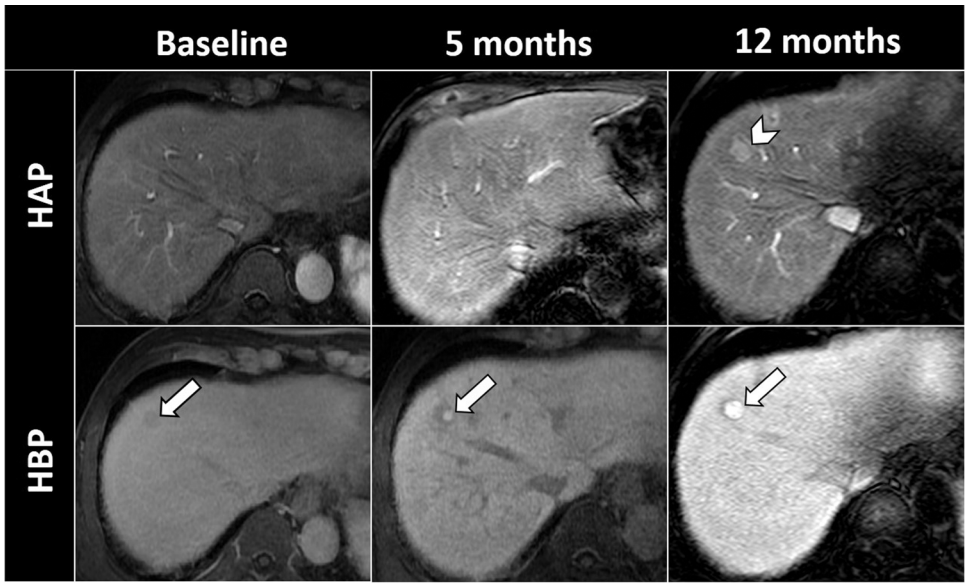

Fig. 4. Serial gadoxetate disodium-enhanced MRI examinations in an 83-year-old male with HCV-related cirrhosis show that nodule-in-nodule hyperintensity on HBP can predate APHE. The baseline MRI shows a nodule without arterial phase hyperenhancement (APHE) and with hypointense signal on the hepatobiliary phase (HBP) (arrow). On the 5-month follow-up, despite the absence of APHE, there is the appearance of a small hyperintense nodule (arrow) on HBP within the larger HBP-hypointense nodule. A 12-month follow-up MRI shows the appearance of APHE (arrowhead) and increase in size of the hyperintense nodule-in-nodule on HBP.

significance of a different paradigm of the classic nodule-in-nodule architecture, manifesting as an inner HBP-hyperintense nodule within a larger outer HBP-hypointense nodule without APHE. In our series 46% of the inner nodules had typical imaging features of HCC with APHE and washout appearance on PVP as opposed to the hypointensity only visualized in the larger outer nodules, a dynamic vascular pattern concordant with the typical description of nodule-in-nodule architecture in prior literature [22–24]. A similar enhancement pattern on HBP was anecdotally described by other authors [25,26]. Similarly to our study, Kobayashi et al. [13] reported that 28.8% of hypervascular foci in a hypovascular nodule, identified on angiography-assisted CT, were hyperintense on HBP compared to the surrounding hypovascular nodules. In addition, Kobayashi et al. [13] described at angiography-assisted CT other patterns of nodule-in-nodule architecture during early-stage of multistep hepatocarcinogenesis including “more hypointense inner nodule in larger hypointense nodule” (8.2%) and “hypointense inner nodule in isointense larger nodule” (12.3%). Although angiography-assisted CT is more accurate for detection of APHE in small nodules, it is an invasive technique that is not routinely performed for nodules follow-up in Western countries. In our study we reported that the hyperintense inner nodule showed APHE in 71%, and its appearance predated that of Liver Imaging Reporting and Data System (LI-RADS) major imaging features [16]. These results support the inclusion of the nodule-in-nodule architecture as an ancillary feature favouring HCC in particular, that may be applied to upgrade LR-3 observation into LR-4 [27].

We also noticed that the hyperintense signal was already visible in 21%, 58% and 83% of nodule-in-nodules on 3-minutes, 5-minutes and 10-minutes phases, respectively. This behavior could be explained by the peculiar pharmacokinetic of gadoxetate disodium with a contrast uptake in the hepatocytes starting as soon as 90 s after the intravenous administration in patients with normal liver function as well as in 9–20% of HCCs [28]. All the included patients were either in Child-Pugh class A or B with relatively preserved liver function as opposed to Child-Pugh C in which the contrast uptake on HBP is known to be significantly impaired [29]. Thus, our results suggest that the hyperintensity of the inner nodule may be already visible on 3-minute transitional phase when imaged with gadoxetate disodium.

We observed restricted diffusion in four out of 13 inner nodules. This finding is not surprising since recent studies have demonstrated that restricted diffusion is a relevant imaging feature for diagnosis of hypovascular HCC and an independent predictive factor for hypervascular transformation of HBP-hypointense nodules without APHE [18,30,31].

The presence of an HBP-hyperintense inner nodule was predating (median 315 days, IQR 124–538 days) the appearance of either APHE or washout on PVP in 12 out of 16 (75%) nodules on subsequent MRI examinations. Thus, the hyperintensity on HPB was the first imaging feature suggesting the progression in the hepatocarcinogenesis process of the HBP-hypointense nodules without APHE. We speculate that the inner nodule on HBP may be used as an additional biomarker for the progression of the multistep carcinogenesis that starts from low-grade dysplastic nodule (LGDN) to high-grade dysplastic nodule (HGDN) or early HCC, and, finally, to HCC development [32]. When a small progressed HCC develops within a larger dysplastic nodule or early HCC, the result is a nodule-in-nodule architecture reflecting the progression in the dedifferentiation of the tumour, replacing part of the larger dysplastic nodule [22,33]. Indeed, the nodule-in-nodule architecture is thought to represent the clonar expansion of a progressed HCC within a dysplastic or early HCC nodule [33,34]. Thus, the entire nodule is pathologically and radiologically classified by the more malignant, less differentiated component [2].

In all of our patients with clinical follow-up available, all the inner nodules underwent locoregional or systemic treatment. A recent study performed by Kang et al. [35] showed a low tumor recurrence rate during long term follow-up after RFA treatment of inner nodules. Conversely, Scheau et al. [36] reported 9 patients with nodule-in-nodule architecture, all with progressive disease on MRI follow-up examination performed one month after TACE. In our population we had two patients with a second nodule-in-nodule architecture appearing as hyperintense on HBP 258 and 459 days after treatment (RFA or TACE, respectively). Although locoregional therapy could be a reasonable treatment option because the nodule-in-nodule architecture represents an early and usually small neoplastic lesion, we believe a short-term follow-up is necessary in these patients due to risk of recurrence and development of HCC associated with those nodules.

Our study has several limitations. First, the number of patients was small. However, this reflects the rarity of this observation. Second, the pathologic analysis of the nodules was not performed and the diagnosis of the lesions was based on the non-invasive MRI criteria only [16,17,37]. Finally, gadoxetate disodium-enhanced MRI may underestimate the presence of APHE compared to CT hepatic arteriography which is more accurate for detection of APHE in nodules smaller than 1 cm. However, this approach better reflects the clinical practice in which invasive procedures are not routinely performed for nodules follow-up. Further studies will be necessary to correlate the expression

of OATP1B3 in HBP-hyperintense inner nodules with the histological progression to HCC.

In conclusion, HBP-hypointense nodules without APHE may contain a smaller HBP-hyperintense inner nodule that can precede the appearance of either APHE or washout on PVP. The nodule-in-nodule architecture on HBP likely represents a focus of progressed HCC within a high-grade dysplastic nodule or early HCC.

Disclosures

Roberto Cannella: not any relevant financial relationships with any commercial interest.

Alberto Calandra: not any relevant financial relationships with any commercial interest.

Giuseppe Cabibbo: not any relevant financial relationships with any commercial interest.

Massimo Midiri: not any relevant financial relationships with any commercial interest.

An Tang: not any relevant financial relationships with any commercial interest.

Giuseppe Brancatelli: lecture fees from Bayer.

Funding

This research did not receive any specific grant from funding agencies in the public, commercial, or not-for-profit sectors.

References

[1] J. Ferlay, I. Soerjomataram, R. Dikshit, S. Eser, C. Mathers, M. Rebelo, D.M. Parkin, D. Forman, F. Bray, Cancer incidence and mortality worldwide: sources, methods and major patterns in GLOBOCAN 2012, Int. J. Cancer 136 (2015) E359–386, https://doi.org/10.1002/ijc.29210.

[2] International Consensus Group for Hepatocellular Neoplasia, Pathologic diagnosis of early hepatocellular carcinoma: a report of the international consensus group for hepatocellular neoplasia, Hepatology 49 (2009) 658–664, https://doi.org/10.1002/hep.22709.

[3] D.G. Mitchell, R. Rubin, E.S. Siegelman, D.L. Burk Jr, M.D. Rifkin, Hepatocellular carcinoma within siderotic regenerative nodules: appearance as a nodule within a nodule on MR images, Radiology 178 (1991) 101–103, https://doi.org/10.1148/radiology.178.1.1845784.

[4] A.G. Sadek, D.G. Mitchell, E.S. Siegelman, E.K. Outwater, T. Matteuccí, H.W. Hann, Early hepatocellular carcinoma that develops within macroregenerative nodules: growth rate depicted at serial MR imaging, Radiology 195 (1995) 753–756, https://doi.org/10.1148/radiology.195.3.7754006.

[5] J.W. Choi, J.M. Lee, S.J. Kim, J.H. Yoon, J.H. Baek, J.K. Han, B.I. Choi, Hepatocellular carcinoma: imaging patterns on gadoxetic acid-enhanced MR Images and their value as an imaging biomarker, Radiology 267 (2013) 776–786, https://doi.org/10.1148/radiol.13120775.

[6] A. Kitao, Y. Zen, O. Matsui, T. Gabata, S. Kobayashi, W. Koda, K. Kozaka, N. Yoneda, T. Yamashita, S. Kaneko, Y. Nakanuma, Hepatocellular carcinoma: signal intensity at gadoxetic acid-enhanced MR Imaging–correlation with molecular transporters and histopathologic features, Radiology 256 (2010) 817–826, https://doi.org/10.1148/radiol.10092214.

[7] M. Narita, E. Hatano, S. Arizono, A. Miyagawa-Hayashino, H. Isoda, K. Kitamura, K. Taura, K. Yasuchika, T. Nitta, I. Ikai, S. Uemoto, Expression of OATP1B3 determines uptake of Gd-EOB-DTPA in hepatocellular carcinoma, J. Gastroenterol. 44 (2009) 793–798, https://doi.org/10.1007/s00535-009-0056-4.

[8] A. Kitao, O. Matsui, N. Yoneda, K. Kozaka, R. Shinmura, W. Koda, S. Kobayashi, T. Gabata, Y. Zen, T. Yamashita, S. Kaneko, Y. Nakanuma, The uptake transporter OATP8 expression decreases during multistep hepatocarcinogenesis: correlation with gadoxetic acid enhanced MR imaging, Eur. Radiol. 21 (2011) 2056–2066, https://doi.org/10.1007/s00330-011-2165-8.

[9] K. Sano, T. Ichikawa, U. Motosugi, H. Sou, A.M. Muhi, M. Matsuda, M. Nakano, M. Sakamoto, T. Nakazawa, M. Asakawa, H. Fujii, T. Kitamura, N. Enomoto, T. Araki, Imaging study of early hepatocellular carcinoma: usefulness of gadoxetic acid-enhanced MR imaging, Radiology 261 (2011) 834–844, https://doi.org/10.1148/radiol.11101840.

[10] Y.S. Kim, J.S. Song, H.K. Lee, Y.M. Han, Hypovascular hypointense nodules on hepatobiliary phase without T2 hyperintensity on gadoxetic acid-enhanced MR images in patients with chronic liver disease: long-term outcomes and risk factors for hypervascular transformation, Eur. Radiol. 26 (2016) 3728–3736, https://doi.org/10.1007/s00330-015-4146-9.

[11] U. Motosugi, T. Murakami, J.M. Lee, K.J. Fowler, J.P. Heiken, C.B. Sirlin, LI-RADS HBA Working Group. Recommendation for terminology: nodules without arterial phase hyperenhancement and with hepatobiliary phase hypointensity in chronic liver disease, J. Magn. Reson. Imaging 48 (2018) 1169–1171, https://doi.org/10.1002/jmri.26515.

[12] C.H. Suh, K.W. Kim, J. Pyo, J. Lee, S.Y. Kim, S.H. Park, Hypervascular transformation of hypovascular hypointense nodules in the hepatobiliary phase of gadoxetic acid-enhanced MRI: a systematic review and meta-analysis, AJR Am. J. Roentgenol. 209 (2017) 781–789, https://doi.org/10.2214/AJR.16.17711.

[13] S. Kobayashi, O. Matsui, T. Gabata, W. Koda, T. Minami, Y. Ryu, K. Kozaka, A. Kitao, Intranodular signal intensity analysis of hypovascular high-risk borderline lesions of HCC that illustrate multi-step hepatocarcinogenesis within the nodule on Gd-EOB-DTPA-enhanced MRI, Eur. J. Radiol. 81 (2012) 3839–3845, https://doi.org/10.1016/j.ejrad.2012.06.027.

[14] E. Neri, M.A. Bali, A. Ba-Ssalamah, P. Boraschi, G. Brancatelli, F.C. Alves, L. Grazioli, T. Helmberger, J.M. Lee, R. Manfredi, L. Martì-Bonmatì, C. Matos, E.M. Merkle, B. Op De Beeck, W. Schima, S. Skehan, V. Vilgrain, C. Zech, C. Bartolozzi, ESGAR consensus statement on liver MR imaging and clinical use of liver-specific contrast agents, Eur. Radiol. 26 (2016) 921–931, https://doi.org/10.1007/s00330-015-3900-3.

[15] Y.J. Suh, M.J. Kim, J.Y. Choi, Y.N. Park, M.S. Park, K.W. Kim, Differentiation of hepatic hyperintense lesions seen on gadoxetic acid-enhanced hepatobiliary phase MRI, AJR Am. J. Roentgenol. 197 (2011) W44–W52, https://doi.org/10.2214/AJR.10.5845.

[16] Liver Imaging Reporting and Data System, American College of Radiology, 2019 Accessed date on May https://www.acr.org/Clinical-Resources/Reporting-and-Data-Systems/LI-RADS.

[17] A. Tang, M.R. Bashir, M.T. Corwin, I. Cruite, C.F. Dietrich, R.K.G. Do, E.C. Ehman, K.J. Fowler, H.K. Hussain, R.C. Jha, A.R. Karam, A. Mamidipalli, R.M. Marks, D.G. Mitchell, T.A. Morgan, M.A. Ohliger, A. Shah, K.N. Vu, C.B. Sirlin, LI-RADS Evidence Working Group, Evidence supporting LI-RADS major features for CT- and MR imaging-based diagnosis of hepatocellular carcinoma: a systematic review, Radiology 286 (2018) 29–48, https://doi.org/10.1148/radiol.2017170554.

[18] H.J. Yang, J.S. Song, E.J. Choi, H. Choi, J.D. Yang, W.S. Moon, Hypovascular hypointense nodules in hepatobiliary phase without T2 hyperintensity: long-term outcomes and added value of DWI in predicting hypervascular transformation, Clin. Imaging 50 (2018) 123–129, https://doi.org/10.1016/j.clinimag.2018.01.003.

[19] T. Inoue, T. Hyodo, T. Murakami, Y. Takayama, A. Nishie, A. Higaki, K. Korenaga, A. Sakamoto, Y. Osaki, H. Aikata, K. Chayama, T. Suda, T. Takano, K. Miyoshi, M. Koda, K. Numata, H. Tanaka, H. Iijima, H. Ochi, M. Hirooka, Y. Imai, M. Kudo, Hypovascular hepatic nodules showing hypointense on the hepatobiliary-phase image of Gd-EOB-DTPA-enhanced MRI to develop a hypervascular hepatocellular carcinoma: a nationwide retrospective study on their natural course and risk factors, Dig. Dis. 31 (2013) 472–479, https://doi.org/10.1159/000355248.

[20] D.R. Ludwig, T.J. Fraum, R. Cannella, D.H. Ballard, R. Tsai, M. Naeem, M. LeBlanc, A. Salter, A. Tsung, A.S. Shetty, A.A. Borhani, A. Furlan, K.J. Fowler, Hepatocellular carcinoma (HCC) versus non-HCC: accuracy and reliability of Liver Imaging Reporting and Data System v2018, Abdom Radiol (NY). 44 (2019) 2116–2132, https://doi.org/10.1007/s00261-019-01948-x.

[21] M. Cerny, C. Bergeron, J.S. Billiard, J. Murphy-Lavallée, D. Olivié, J. Bérubé, B. Fan, H. Castel, S. Turcotte, P. Perreault, M. Chagnon, A. Tang, LI-RADS for MR imaging diagnosis of hepatocellular carcinoma: performance of major and ancillary features, Radiology 288 (2018) 118–128, https://doi.org/10.1148/radiol.2018171678.

[22] J.Y. Choi, J.M. Lee, C.B. Sirlin, CT and MR imaging diagnosis and staging of hepatocellular carcinoma: part II. Extracellular agents, hepatobiliary agents, and ancillary imaging features, Radiology 273 (2014) 30–50, https://doi.org/10.1148/radiol.14132362.

[23] S. Goshima, M. Kanematsu, M. Matsuo, H. Kondo, H. Kato, R. Yokoyama, H. Hoshi, N. Moriyama, Nodule-in-nodule appearance of hepatocellular carcinomas: comparison of gadolinium-enhanced and ferumoxides-enhanced magnetic resonance imaging, J. Magn. Reson. Imaging 20 (2004) 250–255, https://doi.org/10.1002/jmri.20100.

[24] J.S. Yu, J.J. Chung, J.H. Kim, K.W. Kim, Hypervascular focus in the non-hypervascular nodule ("nodule-in-nodule") on dynamic computed tomography: imaging evidence of aggressive progression in hepatocellular carcinoma, J. Comput. Assist. Tomogr. 33 (2009) 131–135, https://doi.org/10.1097/RCT.0b013e3181670fa3.

[25] J.Y. Choi, J.M. Lee, C.B. Sirlin, CT and MR imaging diagnosis and staging of hepatocellular carcinoma: part I. Development, growth, and spread: key pathologic and imaging aspects, Radiology 272 (2014) 635–654, https://doi.org/10.1148/radiol.14132361.

[26] R. Kita, A. Sakamoto, E. Iguchi, H. Takeda, Y. Oohara, N. Nishijima, S. Saito, A. Nasu, H. Nishikawa, T. Kimura, Y. Osaki, T. Wakasa, Y. Nakanuma, O. Matsui, Three cases of hepatocellular carcinoma with nodules showing different signal intensities in the hepatobiliary phase of Gd-EOB-DTPA-enhanced MRI, Nihon Shokakibyo Gakkai Zasshi 111 (2014) 940–947, https://doi.org/10.11405/nisshoshi.111.940.

[27] M. Cerny, V. Chernyak, D. Olivié, J.S. Billiard, J. Murphy-Lavallée, A.Z. Kielar, K.M. Elsayes, L. Bourque, J.C. Hooker, C.B. Sirlin, A. Tang, LI-RADS Version, Ancillary features at MRI, Radiographics 38 (2018) (2018) 1973–2001, https://doi.org/10.1148/rg.2018180052.

[28] T.J. Vogl, S. Kümmel, R. Hammerstingl, M. Schellenbeck, G. Schumacher, T. Balzer, W. Schwarz, P.K. Müller, W.O. Bechstein, M.G. Mack, O. Söllner, R. Felix, Liver tumors: comparison of MR imaging with Gd-EOB-DTPA and Gd-DTPA, Radiology 200 (1996) 59–67, https://doi.org/10.1148/radiology.200.1.8657946.

[29] T. Tamada, K. Ito, A. Higaki, K. Yoshida, A. Kanki, T. Sato, H. Higashi, T. Sone, Gd-EOB-DTPA-enhanced MR imaging: evaluation of hepatic enhancement effects in normal and cirrhotic livers, Eur. J. Radiol. 80 (2011) e311–316, https://doi.org/10.1016/j.ejrad.2011.01.020.

[30] M. Di Pietropaolo, C. Briani, G.F. Federici, M. Marignani, P. Begini, G. Delle Fave,

E. Iannicelli, Comparison of diffusion-weighted imaging and gadoxetic acid-enhanced MR images in the evaluation of hepatocellular carcinoma and hypovascular hepatocellular nodules, Clin. Imaging 39 (2015) 468–475, https://doi.org/10.1016/j.clinimag.2014.12.020.

[31] Y.K. Kim, W.J. Lee, M.J. Park, S.H. Kim, H. Rhim, D. Choi, Hypovascular hypointense nodules on hepatobiliary phase gadoxetic acid-enhanced MR images in patients with cirrhosis: potential of DW imaging in predicting progression to hypervascular HCC, Radiology 265 (2012) 104–114, https://doi.org/10.1148/radiol.12112649.

[32] M. Kudo, Multistep human hepatocarcinogenesis: correlation of imaging with pathology, J. Gastroenterol. 44 (2009) 112–118, https://doi.org/10.1007/s00535-008-2274-6.

[33] M. Kojiro, 'NOdule-in-nodule' appearance in hepatocellular carcinoma: its significance as a morphologic marker of dedifferentiation, Intervirology 47 (2004) 179–183, https://doi.org/10.1159/000078470.

[34] N. Yoneda, O. Matsui, A. Kitao, R. Kita, K. Kozaka, W. Koda, S. Kobayashi, T. Gabata, H. Ikeda, Y. Nakanuma, Hypervascular hepatocellular carcinomas showing hyperintensity on hepatobiliary phase of gadoxetic acid-enhanced magnetic resonance imaging: a possible subtype with mature hepatocyte nature, J. Radiol. 31 (2013) 480–490, https://doi.org/10.1007/s11604-013-0224-6.

[35] T.W. Kang, H. Rhim, K.D. Song, M.W. Lee, D.I. Cha, S.Y. Ha, J.H. Ahn, Radiofrequency ablation of hepatocellular carcinoma with a "Nodule-in-Nodule" appearance: long-term follow-up and clinical implications, Cardiovasc. Intervent. Radiol. 40 (2017) 401–409, https://doi.org/10.1007/s00270-016-1525-9.

[36] A.E. Scheau, C. Scheau, I.G. Lupescu, Nodule-in-Nodule imaging pattern in hepatocellular carcinoma treated by transarterial chemoembolization - a multiparametric magnetic resonance imaging study, J. Gastrointestin. Liver Dis. 26 (2017) 387–393, https://doi.org/10.15403/jgld.2014.1121.264.nin.

[37] J.A. Marrero, L.M. Kulik, C.B. Sirlin, A.X. Zhu, R.S. Finn, M.M. Abecassis, L.R. Roberts, J.K. Heimbach, Diagnosis, staging and management of hepatocellular carcinoma: 2018 practice guidance by the american association for the study of liver diseases, Hepatology 68 (2018) 723–750, https://doi.org/10.1002/hep.29913.